

内蒙古苏崩地点的古新世软食中兽(哺乳纲,中兽目):古新世-始新世界线附近“东方伊甸园”扩散模式的新证据¹⁾

毕丛山¹ 王元青² 孟津^{2,3} 倪喜军^{2,3} Daniel L. GEBO⁴ 李传夔²

(1 美国卡内基自然历史博物馆古脊椎动物学部 匹兹堡 PA 15213)

(2 中国科学院古脊椎动物与古人类研究所,脊椎动物进化系统学重点实验室 北京 100044)

(3 美国自然历史博物馆古生物学部 纽约 10024)

(4 美国北伊利诺伊大学人类学系 迪卡布 60115)

摘要:记述了发现于内蒙古苏崩晚古新世格沙头期的中兽类软食中兽 *Hapalodectes* 属的一个新种。这是软食中兽在中国古新世地层中的首次发现,也是亚洲格沙头期的第二种软食中兽。已有的系统学和生物地层学证据支持软食中兽属和软食中兽科(*Hapalodectidae*)亚洲起源的观点。软食中兽显然是在古新世-始新世极热事件(PETM)期间通过白令陆桥扩散到北美大陆的,因而符合“东方伊甸园”学说中的生物地理格局。软食中兽有限的(即非欧洲的)地理分布使得我们可以重建该属生物地理学历史。如同软食中兽一样的“东方伊甸园”式的扩散模式,可以看作是大的环境变化事件导致多个支系产生相似的系统学和生物地理学分布格局的生物地理扩散机制。严格地检查了所谓的在古新世-始新世界线上或其附近的与“东方伊甸园”模式相矛盾的大陆间哺乳动物扩散事例,结果发现这些例子都是不可靠的。“东方伊甸园”生物地理学说充分解释了PETM时期哺乳动物群更替以及劳亚古陆哺乳动物地理分布格局的成因。

关键词:古新世,始新世,软食中兽,中兽目,生物地理,古新世-始新世极热事件

中图法分类号:Q915.873 文献标识码:A 文章编号:1000-3118(2010)04-0375-15

PALEOCENE HAPALODECTES (MAMMALIA; MESONYCHIA) FROM SUBENG, NEI MONGOL: FURTHER EVIDENCE OF “EAST OF EDEN” DISPERSAL AT THE PALEOCENE-EOCENE BOUNDARY

K. Christopher BEARD^{1*} WANG Yuan-Qing² MENG Jin^{2,3} NI Xi-Jun^{2,3}

Daniel L. GEBO⁴ LI Chuan-Kui²

(1 Section of Vertebrate Paleontology, Carnegie Museum of Natural History 4400 Forbes Avenue, Pittsburgh, PA 15213 USA *email address for corresponding author: beardc@carnegiemnh.org)

(2 Key Laboratory of Evolutionary Systematics of Vertebrates, Institute of Vertebrate Paleontology and Paleoanthropology, Chinese Academy of Sciences Beijing 100044 China)

(3 Division of Paleontology, American Museum of Natural History Central Park West at 79th Street, New York, NY 10024 USA)

(4 Department of Anthropology, Northern Illinois University DeKalb, IL 60115 USA)

1) 国家重点基础研究发展计划项目(编号:2006CB806400)、国家自然科学基金(编号:40532010, 40672009)和美国国家科学基金(编号:EAR-0120727, BCS-0309800, BCS-0820602)资助。

收稿日期:2010-02-28

Abstract A new species of the mesonychian mammal genus *Hapalodectes* is described from the Gashatan (late Paleocene) site of Subeng in Nei Mongol (Inner Mongolia). This is the first Paleocene record of *Hapalodectes* from China, and the second Gashatan species of *Hapalodectes* to be recorded from Asia. Available phylogenetic and biostratigraphic evidence supports an Asian origin for *Hapalodectes* (and Hapalodectidae). *Hapalodectes* apparently dispersed across Beringia coincident with PETM warming to colonize North America, thereby conforming to the “East of Eden” biogeographic pattern. Reconstructing the historical biogeography of *Hapalodectes* is facilitated by its restricted (i. e., non-European) geographic distribution. “East of Eden” dispersal such as that shown by *Hapalodectes* qualifies as an excellent example of geo-dispersal, whereby a major perturbation of the physical environment allows multiple clades to exhibit similar biogeographic and phylogenetic patterns. Purported examples of intercontinental mammalian dispersal at or near the Paleocene–Eocene boundary that conflict with the “East of Eden” pattern are critically examined and found to be wanting. The “East of Eden” biogeographic pattern adequately explains mammalian faunal turnover and Laurasian mammalian biogeography during the PETM.

Key words Paleocene, Eocene, *Hapalodectes*, Mesonychia, biogeography, PETM

1 Introduction

Species of *Hapalodectes* are small mesonychian mammals that range in age from late Paleocene to middle Eocene (Szalay, 1969a; Lopatin, 2001). Like all mesonychians, *Hapalodectes* is distinctive in having buccolingually compressed lower cheek teeth with talonids that are simplified to include little more than the cristid obliqua and the hypoconid (Szalay, 1969b). However, even among mesonychians, the degree to which the lower cheek teeth of *Hapalodectes* are buccolingually compressed is extreme. Upper molars of *Hapalodectes* are unique among mesonychians in having hypocones, and the cranial morphology of *Hapalodectes* differs from that of mesonychid mesonychians in having a postorbital bar, a relatively expanded neurocranium and a relatively short face (Ting and Li, 1987). These morphological differences are reflected in recent phylogenetic reconstructions of mesonychian relationships, which recognize Hapalodectidae (including *Hapalodectes* and the poorly documented *Hapalorestes*) as the sister group of Mesonychidae (Geisler and McKenna, 2007). Such a basal phylogenetic position for Hapalodectidae within Mesonychia implies that the group diverged from Mesonychidae no later than the early Paleocene, well before its first appearance in the fossil record. Szalay (1969a) anticipated such an early divergence date for Hapalodectidae decades before Paleocene records of the group were actually discovered.

The documented geographic range of Hapalodectidae includes China and Mongolia in eastern Asia (Matthew and Granger, 1925; Li and Ting, 1987; Lopatin, 2001; Tong and Wang, 2006) and Wyoming and Colorado in western North America (Matthew, 1909, 1915; Gazin, 1962; Szalay, 1969a; Zhou and Gingerich, 1991; O’Leary and Rose, 1995; Gunnell and Gingerich, 1996; O’Leary, 1998). Hapalodectid mesonychians have never been reported from Europe. The apparent absence of hapalodectids from the early Cenozoic record of Europe stands in contrast to the generally cosmopolitan nature of Laurasian mammal faunas at that time, and particularly during the early Eocene. Beard and Dawson (1999) cited the restricted geographic occurrence of Hapalodectidae within Laurasia as one line of evidence suggesting that direct dispersal between eastern Asia and western Europe was not feasible during the latest Paleocene and earliest Eocene.

Faunal turnover at the Paleocene–Eocene boundary was profound across Laurasia, when members of such modern orders of mammals as Artiodactyla, Perissodactyla and Primates appeared more or less synchronously across all three Holarctic continents (Gingerich, 1989; Krause and Maas, 1990; Hooker, 1998; Beard, 1998, 2008; Beard and Dawson, 1999, 2009; Bowen et al., 2002; Ni et al., 2004, 2005; Gingerich and Smith, 2006; Smith et al., 2006). However, early members of these extant orders of mammals were not the only mammalian

taxa to disperse widely at this time. Other members of this wave of immigrant taxa included the extinct Hyaenodontidae (order Creodonta) and Hapalodectidae (order Mesonychia). Although hyaenodontids are frequently cited in discussions of mammalian dispersal and faunal change at the Paleocene–Eocene boundary (Gingerich, 1989; Krause and Maas, 1990; Hooker, 1998; Gingerich and Smith, 2006), hapalodectids have only rarely been mentioned in this context (Beard and Dawson, 1999).

The nearly synchronous pattern of mammalian turnover at the Paleocene–Eocene boundary has complicated attempts to reconstruct the dispersal history and biogeographic origins of the higher-level mammalian taxa that then became widespread. Gondwanan origins for some or all of these taxa have been proposed repeatedly (Gingerich, 1989; Krause and Maas, 1990; Hooker, 1998; Solé et al., 2009), although this possibility has been disputed on both phylogenetic and biostratigraphic grounds (Beard, 1998, 2006; Beard and Dawson, 1999). Even within Laurasia, the dispersal history of various mammals at the Paleocene–Eocene boundary is reconstructed differently by different workers (Beard and Dawson, 1999; Hooker and Dashzeveg, 2003; Ni et al., 2005; Smith et al., 2006; Beard, 2008).

Given that hapalodectids have played a very limited role in previous discussions of mammalian dispersal at the Paleocene–Eocene boundary, the purpose of this paper is threefold. First, we describe the only Paleocene record of *Hapalodectes* from China and assess its phylogenetic position with respect to other species of the genus. Second, we reconstruct the likely dispersal history of Hapalodectidae, based on available biostratigraphic and phylogenetic data for the family. Finally, we examine how the hapalodectid record affects reconstructions of the dispersal history of other mammalian taxa near the Paleocene–Eocene boundary.

2 Systematic paleontology

Class Mammalia Linnaeus, 1758

Supercohort Theria Parker & Haswell, 1897

Cohort Placentalia Owen, 1837

Order Mesonychia Matthew, 1909

Family Hapalodectidae Szalay & Gould, 1966

Genus *Hapalodectes* Matthew, 1909

Hapalodectes paleocenus sp. nov.

Holotype IVPP V 14713, left dentary fragment bearing the crowns of m2–3 (Fig. 1).

Hypodigm The holotype (only known specimen).

Type locality Subeng (43°31'49.80" N, 111°44'7.08" E), Nei Mongol (Inner Mongolia), about 25 km west of Erlian.

Known distribution Gashatan (late Paleocene) Nomogen Formation, Erlian Basin, Nei Mongol, China.

Diagnosis Smaller than *H. leptognathus*, *H. huanghaiensis* and *H. serus*; larger than *H. hetangensis*. Differs from *Hapalodectes dux*, *H. hetangensis*, and *H. huanghaiensis* in having weaker metaconids on its lower molars. Differs from *H. anthracinus* and *H. serus* in having stronger metaconids on its lower molars.

Etymology Trivial name recognizes the Paleocene age of this species.

Description The dentary is relatively shallow and uniform in depth (7.80 mm below the talonid of m3) throughout its preserved length. Medially, a longitudinally oriented groove marking the area for the origin of the mylohyoid muscle runs near the inferior margin of the dentary. Laterally, the deeply excavated masseteric fossa extends forward to a point lying beneath the talonid of m3. Neither the coronoid process nor the condyle is preserved.

The m2 (length, 4.20 mm; width 1.65 mm) is relatively low-crowned, and its trigonid is

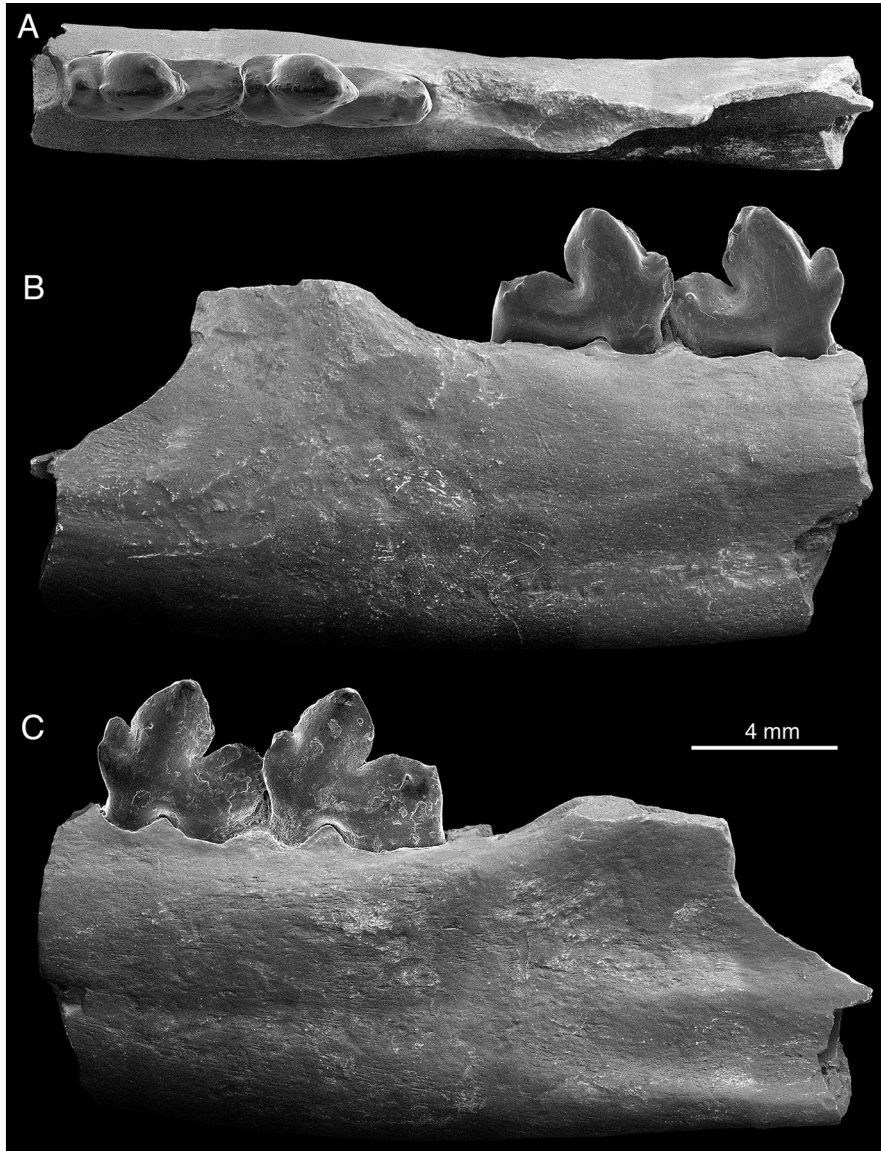


Fig. 1 *Hapalodectes paleocenus* sp. nov., holotype left dentary fragment bearing m2–3 (IVPP V 14713)
A. occlusal view; B. lingual view; C. buccal view

canted slightly posteriorly. The tall, voluminous protoconid is flanked anteriorly and posteriorly by the weakly developed pre- and postprotocristid, respectively. The angle at which these trigonid crests diverge from one another is relatively wide (approximating a right angle), as is also the case in *H. dux*. The preprotocristid follows an arcuate trajectory down the leading edge of the trigonid, terminating in a notch at the posterior base of the paraconid. The latter cusp is relatively small and anteroposteriorly short. Directly anterior to the paraconid, but closer to the base of the crown, is the reentrant groove that accommodates the talonid of m1. Minute cuspules occur on either side of the reentrant groove. Lingual to the preprotocristid and running parallel to it, a furrow separates a small metaconid from the adjacent protoconid. The metaconid is nearly connate with the protoconid, being situated anterolingual to the latter cusp and slightly lower.

An obliquely oriented crest joins the apices of the metaconid and protoconid. The post-protocristid traces an arcuate path down the posterior edge of the trigonid before meeting the cristid obliqua at a well-defined notch near the junction of the trigonid and talonid. The cristid obliqua is relatively low, reaching its highest point near the center of its anteroposterior length, at a location that probably marks the position of the hypoconid. If present, the hypoconulid was vestigial. A tiny cuspule occurs on the lingual side of the talonid in a position appropriate for the entoconid.

The m3 (length, 4.70 mm; width 1.70 mm) closely resembles m2 in terms of overall morphology. It differs from the latter tooth chiefly in having a longer talonid. The cristid obliqua of m3 appears to be slightly lower than that of m2, and it bears two diminutive cuspules near its posterior terminus. Three additional cuspules occur both buccal (one) and lingual (two) to the cristid obliqua.

Comparisons Given their similar age, it is perhaps not surprising that *Hapalodectes paleocenus* closely resembles *H. dux*, known from the Gashatan Zhigden Member of the Naran Bulak Formation in the Nemegt Basin of southern Mongolia (Lopatin, 2001). These two Gashatan species of *Hapalodectes* are similar in size, but they differ in lower molar morphology and molar proportions. *H. dux* has prominent metaconids on its lower molars and its m3 is similar in length to m2, whereas *H. paleocenus* has weakly developed metaconids on its lower molars and its m3 is approximately 12% longer than its m2. Given the simplified structure of the lower molars in *Hapalodectes*, these differences appear to be systematically informative. Indeed, similar characters are widely used to distinguish Eocene species of *Hapalodectes* (Ting and Li, 1987; Zhou and Gingerich, 1991; Tong and Wang, 2006).

Two species of *Hapalodectes* have been reported from the Bumbanian of China: *H. hetangensis* from the Lingcha local fauna of Hunan Province (Ting and Li, 1987) and *H. huanghaiensis* from the Wutu local fauna of Shandong Province (Tong and Wang, 2006). *H. paleocenus* differs from these younger species of *Hapalodectes* in both size and molar morphology. In contrast to *H. paleocenus*, both *H. hetangensis* and *H. huanghaiensis* bear well-developed metaconids on their lower molars. *H. paleocenus* is intermediate in size between the two Bumbanian species of *Hapalodectes*, being larger than *H. hetangensis* but smaller than *H. huanghaiensis*. *H. hetangensis* further differs from *H. paleocenus* in having m3 slightly shorter than m2, thereby being more similar to *H. dux* than to *H. paleocenus* in terms of lower molar proportions. The lower molar talonids of *H. huanghaiensis* differ from those of *H. paleocenus* in bearing two distinct cusps (probably hypoconid and hypoconulid) on the cristid obliqua, which becomes progressively taller posteriorly, rather than reaching its highest point near its midline as is the case in *H. paleocenus*. The lower molar trigonids of *H. huanghaiensis* are taller, more acute, and more vertically oriented than those of *H. paleocenus*.

Hapalodectes serus from the Irдинmanhan of Nei Mongol and *H. anthracinus* from the early Wasatchian of Wyoming differ from *H. paleocenus* in lacking any trace of lower molar metaconids. *H. anthracinus* further differs from *H. paleocenus* in many of the same lower molar characters that distinguish Bumbanian *H. huanghaiensis* from *H. paleocenus*. Like *H. huanghaiensis*, *H. anthracinus* has taller, more acute, and more nearly vertical molar trigonids than does *H. paleocenus*. Likewise, the lower molar talonid crests in *H. anthracinus* are tallest posteriorly, in contrast to the condition in *H. paleocenus*. *H. anthracinus* and *H. paleocenus* are similar in size, but *H. serus* is significantly larger.

The type species of *Hapalodectes*, *H. leptognathus* from the Wasatchian of Wyoming and Colorado, remains relatively poorly known (Szalay, 1969a; O'Leary, 1998). *H. leptognathus* is substantially larger than *H. paleocenus*, but both species retain weakly developed metaconids on their lower molars. *H. leptognathus* differs from *H. paleocenus* in having relatively longer paraconids on its lower molars and in having lower molar talonid crests that are tallest posteriorly.

3 Phylogenetic analysis

Aside from a general consensus that hapalodectids comprise a monophyletic group that probably constitutes the sister taxon of Mesonychidae (Szalay, 1969a; Geisler and McKenna, 2007), relatively few hypotheses have been proposed regarding hapalodectid relationships. Zhou and Gingerich (1991) hypothesized that *H. anthracinus* from the Wasatchian of Wyoming and *H. serus* from the Irдинmanhan of Nei Mongol might pertain to a single lineage, based on their shared, derived loss of lower molar metaconids. Relying heavily on biostratigraphic data, Lopatin (2001) suggested that *Hapalodectes dux* from the Gashatan late Paleocene of southern Mongolia “is a plesiomorphic taxon in relation to all Eocene species of *Hapalodectes* and may be their common ancestor.”

In an attempt to clarify the relationships among species of *Hapalodectes*, we expanded and modified the character-taxon matrix published by Geisler and McKenna (2007) to include additional dental characters and all currently recognized species of *Hapalodectes*. This revised data matrix includes 24 taxa scored for 97 morphological characters, 37 of which are multistate characters that were treated as “ordered” for purposes of parsimony analysis (Appendices 1–2).

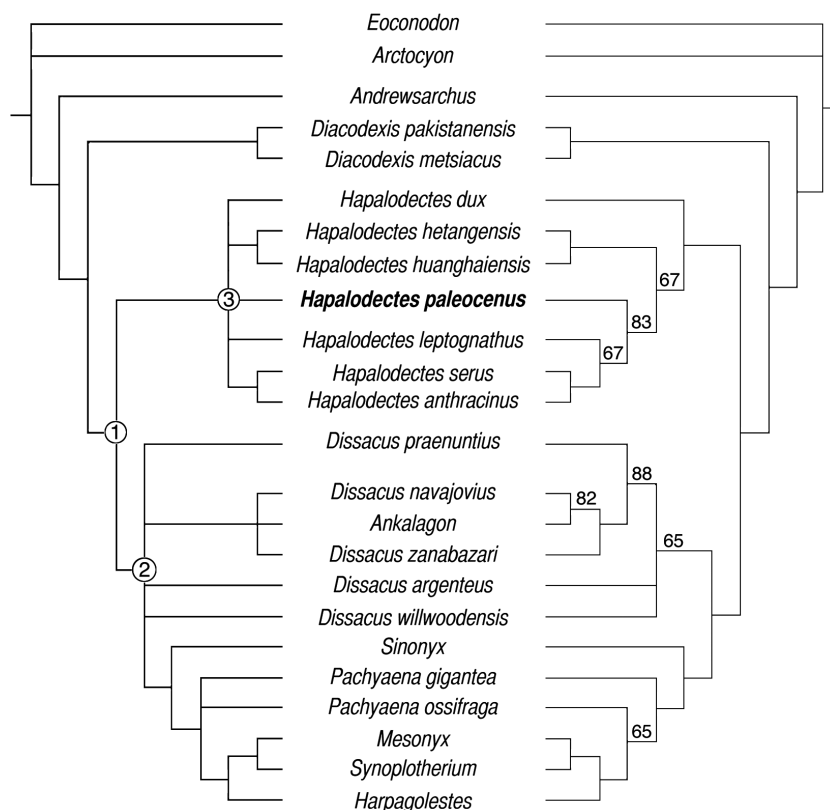


Fig. 2 Strict consensus tree (left) and 50% majority-rule consensus tree (right) summarizing phylogenetic relationships among mesonychians and selected outgroups, based on 102 most parsimonious trees (MPTs) recovered from analysis of the character-taxon matrix shown in Appendix 2 (see text for further details). For the strict consensus tree, node 1 = Mesonychia, node 2 = Mesonychidae, and node 3 = Hapalodectidae; for the 50% majority-rule consensus tree, the numbers above selected branches show the percentage of MPTs consistent with the more highly-resolved topology than that of the strict consensus tree

All character state transformations were weighted equally. We analyzed the data matrix using the branch-and-bound search criterion in PAUP 4.0b10 (Swofford, 2002), which guarantees the recovery of all most parsimonious trees (MPTs). 102 MPTs were recovered, each having a tree length of 257 and a consistency index of 0.5603. A strict consensus tree that summarizes the phylogenetic resolution obtained by our analysis is depicted in Fig. 2.

The topology supported by our strict consensus tree corresponds closely to that reported by Geisler and McKenna (2007, fig. 12), as would be expected given the general similarity of the data matrices and phylogenetic methods employed in both analyses. In particular, Mesonychia (without *Andrewsarchus*) is recovered as a clade that includes the sister taxa Mesonychidae and Hapalodectidae. Within *Hapalodectes*, our analysis yielded relatively little phylogenetic resolution. The two Chinese Bumbanian species, *Hapalodectes hetangensis* and *H. huanghaiensis*, appear to be sister taxa. Likewise, the two species of *Hapalodectes* characterized by the loss of lower molar metaconids, *H. anthracinus* and *H. serus*, appear to be sister taxa. Both Paleocene species of *Hapalodectes*, as well as *H. leptognathus* from the Wasatchian of North America, join the prior two clades to form an unresolved polytomy.

4 Discussion

Dispersal history of *Hapalodectes* Highly corroborated hypotheses regarding the historical biogeography of a given taxon are supported by both biological (phylogenetic) and geological (biostratigraphic and/or geochronological) data (Beard, 1998). In the case of *Hapalodectes*, phylogenetic resolution at the species level remains poor, as might be expected given the meager anatomical documentation available for most species of this genus. Based on the phylogenetic analysis performed here, the most basal node within *Hapalodectes* is an unresolved polytomy consisting of five clades (Fig. 2). Three of these five clades (*H. dux*, *H. paleocenus*, and the *H. hetangensis* + *H. huanghaiensis* clade) show an Asian distribution, one (*H. leptognathus*) shows a North American distribution, and the remaining one (*H. serus* + *H. anthracinus*) is distributed on both sides of the North Pacific. Examination of the 50% majority-rule consensus based on the 102 MPTs recovered from this analysis provides modest phylogenetic support for an Asian origin of *Hapalodectes*. In 67% of all MPTs, North American *H. leptognathus* is recovered as the sister group of the *H. anthracinus* + *H. serus* clade. This putative clade (including both North American species of *Hapalodectes* as well as *H. serus* from the Irindinmanhan of Asia) is nested deeply within the *Hapalodectes* radiation, with the three exclusively Asian clades occupying successively more basal nodes on the 50% majority-rule consensus tree (Fig. 2).

Prior to the discovery of Paleocene records of *Hapalodectes* in Mongolia and China, *H. anthracinus* (from early Wasatchian zones Wa-1 and Wa-2) was thought to be the oldest known species of *Hapalodectes* (Zhou and Gingerich, 1991). However, intercontinental correlation based on the carbon isotope excursion at the Paleocene–Eocene boundary indicates that *H. hetangensis* from the Bumbanian Lingcha local fauna of Hunan Province, China is clearly older than *H. anthracinus* from early Wasatchian strata in the Bighorn Basin of Wyoming (Bowen et al., 2002; Ting et al., 2003; Smith et al., 2006; Beard, 2008). A second Bumbanian species of *Hapalodectes*, *H. huanghaiensis* from the Wutu local fauna of Shandong Province, China, is plausibly older than *H. hetangensis* on biostratigraphic grounds (Beard, 1998; Beard and Dawson, 1999; Bowen et al., 2002; for a contrary view, see Tong and Wang, 2006), although independent geochronological data that might be used to test this hypothesis are currently lacking.

Hapalodectes dux from the Gashatan of Mongolia and *H. paleocenus* from the Gashatan of Nei Mongol, China are the only Paleocene records of *Hapalodectes* currently known. Although the Paleocene age of Asian Gashatan faunas is now widely accepted (Wang et al., 1998, 2007;

Meng et al., 1998, 2007a,b; Missiaen and Smith, 2008), more precise correlation of the Gashatan with the North American sequence of Paleocene land mammal ages and faunal zones remains contentious. For example, Ting (1998) considered the Gashatan as being correlative with the Clarkforkian, while Solé et al. (2009:827) simply called it “latest Paleocene.” Others have suggested that the Gashatan probably correlates with older Paleocene faunas in North America, specifically the late Tiffanian and early Clarkforkian (Beard, 1998; Wang et al., 1998, 2007; Beard and Dawson, 1999; Meng et al., 2007a). Recently published paleomagnetic data from the Nomogen Formation in the Erlian Basin support an older correlation for the Gashatan, because Gashatan faunas locally occur near the base of Chron C25r (Sun et al., 2009). These paleomagnetic data indicate that Gashatan faunas from the Erlian Basin correlate near the boundary between the late Tiffanian Ti4 and Ti5 faunal zones of western North America (roughly 58.3 Ma, based on the work of Secord et al., 2006). Accordingly, the oldest Asian records of *Hapalodectes*, in the form of *H. dux* and *H. paleocenus*, are likely to be roughly 2.5 Ma older than the earliest known North American record of this taxon (*H. anthracinus*).

Given the clear disparity in age between the earliest Asian and North American records of *Hapalodectes*, and in light of the modest support for a relatively basal phylogenetic position of various Asian species of *Hapalodectes* with respect to their North American relatives, an Asian origin for *Hapalodectes* (and Hapalodectidae) is supported here. In the well-documented Paleocene–Eocene boundary interval of the Bighorn Basin in Wyoming, Hapalodectidae first appear in early Wasatchian (Wa-1) strata (Zhou and Gingerich, 1991; O’Leary and Rose, 1995). After originating in Asia, *Hapalodectes* probably dispersed across Beringia at or near the Paleocene–Eocene boundary. Assuming that Asian *H. serus* is specially related to North American *H. anthracinus* (Fig. 2), a subsequent lineage of *Hapalodectes* likely dispersed in the opposite direction (from North America to Asia) sometime during the early middle Eocene.

Broader biogeographic implications Mammalian dispersal across Laurasia was pervasive enough during the earliest Eocene to establish a nearly cosmopolitan fauna encompassing much of the Holarctic region. Because of the taxonomic breadth and nearly synchronous timing of these intercontinental dispersal events, no consensus has emerged regarding where these mammals originated, nor is there agreement on how they achieved their broad distribution. Rapid and dramatic warming at the Paleocene–Eocene boundary would have facilitated dispersal across high latitude land bridges connecting Asia with North America and North America with Europe (Beard and Dawson, 1999; Beard, 2008). Various authors have suggested that direct dispersal between Asia and Europe was also feasible during the earliest Eocene (Hooker and Dashzeveg, 2003; Smith et al., 2006), but this possibility remains controversial because the Turgai Straits would have posed a significant marine barrier to terrestrial mammals during this time of relatively high eustatic sea level (Woodburne and Swisher, 1995; Beard, 2008).

The restricted geographic range of *Hapalodectes* during the early Cenozoic severely limits the number of biogeographic hypotheses that can be proposed to explain its distribution. We interpret the available geological and biological data as strongly supporting dispersal of *Hapalodectes* from Asia to North America at or near the Paleocene–Eocene boundary (see above). This eastward, trans-Beringian dispersal pattern was dubbed “East of Eden” dispersal by Beard (1998), who thought it corresponded to a taxonomically more extensive and temporally more enduring pattern of dispersal, at least during the early Cenozoic.

What, if anything, does the “East of Eden” dispersal pattern shown by *Hapalodectes* near the Paleocene–Eocene boundary imply about the more general issue of mammalian dispersal across Laurasia at this time? The choice basically comes down to whether one prefers simple, more parsimonious biogeographic hypotheses as opposed to more complicated, helter-skelter dispersal scenarios. The simplest interpretation of mammalian dispersal across Laurasia at the Paleocene–Eocene boundary is that *Hapalodectes* dispersed alongside a taxonomically broad assem-

blage of mammals that exhibited a surprising range of ecological preferences. According to this hypothesis, hapalodectids, hyaenodontids, perissodactyls, artiodactyls, and primates dispersed *en suite* across Beringia from Asia to North America. With the notable exception of *Hapalodectes*, these taxa then proceeded across the North Atlantic land bridge to colonize western Europe (Beard, 1998, 2008; Beard and Dawson, 1999). Biostratigraphic evidence clearly supports this dispersal pattern in the case of hapalodectids and hyaenodontids, both of which show Gashatan first appearances in Asia and Eocene first appearances in North America and/or Europe (Meng et al., 1998). Less obvious, but still significant, biostratigraphic evidence supports a similar dispersal pattern for primates at the Paleocene–Eocene boundary (Beard, 2008). The case for artiodactyls and perissodactyls is less convincing, although both taxa are represented in Asia by putative Paleocene records or closely related outgroups (McKenna et al., 1989; Meng et al., 1998; Ting et al., 2007). Neither of these taxa appears in North America or Europe until the Eocene.

Lieberman (2003) refers to congruent patterns of dispersal among multiple clades as geo-dispersal, and he notes that such congruent phylogenetic and biogeographic patterns resemble those that have long been sought by vicariance biogeographers. In many ways, geo-dispersal is the logical antithesis of vicariance, although both phenomena arise as a result of large-scale perturbations of the physical environment caused by, for example, tectonic or climatic changes. “East of Eden” dispersal at the Paleocene–Eocene boundary qualifies as an excellent example of geo-dispersal because it applies to multiple clades and because the perturbation of the physical environment that induced geo-dispersal is well known, being equivalent to the rapid and dramatic episode of global warming known as the Paleocene – Eocene Thermal Maximum (PETM). More generally, the “East of Eden” biogeographic pattern corresponds to an iterative succession of geo-dispersal events that was apparently controlled by oscillating bouts of climatic change through time (Beard, 1998, 2008; Beard and Dawson, 1999).

Evolutionary biologists search for repeating patterns in nature because such patterns have the potential to yield insights that transcend the random noise of chance events. Nevertheless, random events have obviously occurred throughout the history of life. Did such random episodes of dispersal significantly affect mammalian distributional patterns near the Paleocene–Eocene boundary? Various authors have made this claim, but few instances of intercontinental mammalian dispersal aside from those that conform to the “East of Eden” pattern have been substantiated. Part of the problem stems from the related issues of causality and synchronicity. Geo-dispersal caused by PETM warming adequately explains how a wave of mammalian immigrants hailing from Asia could have successively colonized North America and Europe by traversing high latitude land bridges that suddenly became viable pathways for dispersal because of the rapidly ameliorating climate. It also explains how some taxa could have dispersed in the opposite direction, either from Europe to North America or from North America to Asia, at the same time. Synchronous dispersal across other routes requires a different causal mechanism than PETM warming. Possibilities include the tectonic collision between India and Asia (Krause and Maas, 1990) and a rapid drop in eustatic sea level that would have facilitated direct overland dispersal from Asia to Europe or vice versa (Smith et al., 2006).

Unless one postulates some causal link between PETM warming and either the India-Asia collision or a rapid drop in eustatic sea level, the chance that such events might have occurred synchronously would appear to be vanishingly small. Recent geological studies of the suture zone between Tibet and India suggest that collision between India and Asia occurred tens of millions of years after the PETM, near the end of the Eocene (Ali and Aitchison, 2008). An older collision between India and an intra-oceanic island arc located far to the south of Tibet may have occurred near the Paleocene–Eocene boundary, allowing for limited biotic interchange between Asia and India at this time (Ali and Aitchison, 2008). Paleontological data from the

Ghazij Formation in Pakistan indicate that an endemic mammalian fauna inhabited the Indian plate during the earliest Eocene (Clyde et al., 2003). The local first appearance of perissodactyls and other distinctively Eocene Laurasian mammal taxa occurred later, but still during the early Eocene, suggesting dispersal of these forms into India from Asia rather than vice versa as Krause and Maas (1990) originally posited.

Smith et al. (2006) suggested that multiple mammalian clades, including primates, artiodactyls, and hyaenodontids, dispersed from Asia to Europe to North America near the Paleocene–Eocene boundary, a dispersal pathway that conflicts with the “East of Eden” pattern. Several problems, both theoretical and empirical, weigh on this hypothesis. As noted earlier, dispersal along pathways other than the high latitude corridors linking Asia with North America and North America with Europe must rely upon some causal mechanism other than PETM warming per se. Smith et al. (2006) cite a major episode of sea level lowering as a key factor mitigating westward dispersal of mammals from Asia to Europe. However, the significant episode of marine regression to which these authors refer (the TP 2.3/TE 1.1 sequence boundary of Baum and Vail, 1988) apparently postdates the Paleocene–Eocene boundary (Beard and Dawson, 2009). Likewise, according to Smith et al. (2006) an important subset of the mammalian taxa that colonized North America at the beginning of the Eocene dispersed westward across Eurasia prior to crossing the North Atlantic land bridge, while others, such as perissodactyls (and presumably hapalodectids) followed the more conventional “East of Eden” route to colonize North America directly from Asia. Not only is this biogeographic reconstruction inherently more complicated than that which is preferred here, it fails to explain how both sets of taxa, one hailing from the east and the other hailing from the west, arrived in North America at the same time. Finally, the recent description of the earliest Wasatchian Red Hot local fauna from the Gulf Coastal Plain of Mississippi indicates that the earliest records of North American primates, artiodactyls, and hyaenodontids slightly antedate the oldest records of these taxa in Europe (Beard and Dawson, 2009). This finding obviates any need to resort to overly complicated dispersal scenarios for Laurasian mammals at the Paleocene–Eocene boundary. The “East of Eden” pattern of dispersal appears adequate to explain mammalian faunal turnover at the Paleocene–Eocene boundary in North America.

Acknowledgements We thank B. Bai, Q. Cao, W. Gao, X. Jin, C. Li, P. Li, Qian Li, Qiang Li, S.-J. Li, C.-K. Sun, and R. Yang of IVPP and T.-Y. Wang of Peking University for their assistance in the field. Our fieldwork in early Cenozoic strata of the Erlian Basin is jointly funded by the National Natural Science Foundation of China (grant 40532010, 40672009), the Major Basic Research Projects of MST of China (2006CB806400), and the U. S. National Science Foundation (EAR-0120727, BCS-0309800, BCS-0820602).

References

- Ali J R, Aitchison J C, 2008. Gondwana to Asia: plate tectonics, paleogeography and the biological connectivity of the Indian sub-continent from the Middle Jurassic through latest Eocene (166–35 Ma). *Earth Sci Rev*, **88**: 145–166
- Baum G R, Vail P R, 1988. Sequence stratigraphic concepts applied to Paleogene outcrops, Gulf and Atlantic basins. In: Wilgus C K ed. *Sea-Level Changes — an Integrated Approach*. SEPM Spec Publ, **42**: 309–327
- Beard K C, 1998. East of Eden: Asia as an important center of taxonomic origination in mammalian evolution. *Bull Carnegie Mus Nat Hist*, **34**: 5–39
- Beard K C, 2006. Mammalian biogeography and anthropoid origins. In: Lehman S M, Fleagle J G eds. *Primate Biogeography*. New York: Springer. 439–467
- Beard K C, 2008. The oldest North American primate and mammalian biogeography during the Paleocene–Eocene thermal maximum. *Proc Natl Acad Sci*, **105**: 3815–3818

- Beard K C, Dawson M R, 1999. Intercontinental dispersal of Holarctic land mammals near the Paleocene/Eocene boundary: paleogeographic, paleoclimatic and biostratigraphic implications. *Bull Soc Géol Fr*, **170**: 697–706
- Beard K C, Dawson M R, 2009. Early Wasatchian mammals of the Red Hot local fauna, uppermost Tuscaloosa Formation, Lauderdale County, Mississippi. *Ann Carnegie Mus*, **78**: 193–243
- Bowen G J, Clyde W C, Koch P L et al., 2002. Mammalian dispersal at the Paleocene/Eocene boundary. *Science*, **295**: 2062–2065
- Clyde W C, Khan I H, Gingerich P D, 2003. Stratigraphic response and mammalian dispersal during initial India-Asia collision: evidence from the Ghazij Formation, Balochistan, Pakistan. *Geology*, **31**: 1097–1100
- Gazin C L, 1962. A further study of the Lower Eocene mammalian faunas of southwestern Wyoming. *Smithson Misc Collns*, **144**: 1–98
- Geisler J H, McKenna M C, 2007. A new species of mesonychian mammal from the lower Eocene of Mongolia and its phylogenetic implications. *Acta Palaeont Pol*, **52**: 189–212
- Gingerich P D, 1989. New earliest Wasatchian mammalian fauna from the Eocene of northwestern Wyoming: composition and diversity in a rarely sampled high-floodplain assemblage. *Univ Mich Pap Paleontol*, **28**: 1–97
- Gingerich P D, Smith T, 2006. Paleocene–Eocene land mammals from three new late Clarkforkian and earliest Wasatchian wash sites at Polecat Bench in the northern Bighorn Basin, Wyoming. *Contrib Mus Paleont Univ Mich*, **31**: 245–303
- Gunnell G F, Gingerich P D, 1996. New hapalodectid *Hapalorestes lovei* (Mammalia, Mesonychia) from the early middle Eocene of northwestern Wyoming. *Contrib Mus Paleont Univ Mich*, **29**: 413–418
- Hooker J J, 1998. Mammalian faunal change across the Paleocene–Eocene transition in Europe. In: Aubry M-P, Lucas S G, Berggren W A eds. *Late Paleocene–Early Eocene Climatic and Biotic Events in the Marine and Terrestrial Records*. New York: Columbia University Press. 428–450
- Hooker J J, Dashzeveg D, 2003. Evidence for direct mammalian faunal interchange between Europe and Asia near the Paleocene–Eocene boundary. *Geol Soc Am Spec Pap*, **369**: 479–500
- Krause D W, Maas M C, 1990. The biogeographic origins of late Paleocene–early Eocene mammalian immigrants to the Western Interior of North America. *Geol Soc Am Spec Pap*, **243**: 71–105
- Lieberman B S, 2003. Paleobiogeography: the relevance of fossils to biogeography. *Ann Rev Ecol Evol Syst*, **34**: 51–69
- Lopatin A V, 2001. The earliest *Hapalodectes* (Mesonychia, Mammalia) from the Paleocene of Mongolia. *Paleont J*, **35**: 426–432
- Matthew W D, 1909. The Carnivora and Insectivora of the Bridger Basin, middle Eocene. *Mem Am Mus Nat Hist*, **9**: 289–567
- Matthew W D, 1915. A revision of the Lower Eocene Wasatch and Wind River faunas. Part 1. Order Ferae (Carnivora). Suborder Creodonta. *Bull Am Mus Nat Hist*, **34**: 1–103
- Matthew W D, Granger W, 1925. New mammals from the Irдин Manha Eocene of Mongolia. *Am Mus Novit*, (198): 1–10
- McKenna M C, Chow M C, Ting S Y et al., 1989. *Radinskya yupingae*, a perissodactyl-like mammal from the late Paleocene of China. In: Prothero D R, Schoch R M eds. *The Evolution of Perissodactyls*. New York: Oxford University Press. 24–36
- Meng J, Ni X J, Li C K et al., 2007a. New material of Alagomyidae (Mammalia, Glires) from the late Paleocene Subeng locality, Inner Mongolia. *Am Mus Novit*, (3597): 1–29
- Meng J, Wang Y Q, Ni X J et al., 2007b. New stratigraphic data from the Erlian Basin: implications for the division, correlation, and definition of Paleogene lithological units in Nei Mongol (Inner Mongolia). *Am Mus Novit*, (3570): 1–31
- Meng J, Zhai R J, Wyss A R, 1998. The late Paleocene Bayan Ulan fauna of Inner Mongolia, China. *Bull Carnegie Mus Nat Hist*, **34**: 148–185
- Missiaen P, Smith T, 2008. The Gashatan (late Paleocene) mammal fauna from Subeng, Inner Mongolia, China. *Acta Palaeont Pol*, **53**: 357–378
- Ni X J, Hu Y M, Wang Y Q et al., 2005. A clue to the Asian origin of euprimates. *Anthrop Sci*, **113**: 3–9

- Ni X J, Wang Y Q, Hu Y M et al., 2004. A euprimate skull from the early Eocene of China. *Nature*, **427**: 65–68
- O’Leary M A, 1998. Morphology of the humerus of *Hapalodectes* (Mammalia, Mesonychia). *Am Mus Novit*, (3242): 1–6
- O’Leary M A, Rose K D, 1995. New mesonychian dentitions from the Paleocene and Eocene of the Bighorn Basin, Wyoming. *Ann Carnegie Mus*, **64**: 147–172
- Secord R, Gingerich P D, Smith M E et al., 2006. Geochronology and mammalian biostratigraphy of middle and upper Paleocene continental strata, Bighorn Basin, Wyoming. *Am J Sci*, **306**: 211–245
- Smith T, Rose K D, Gingerich P D, 2006. Rapid Asia–Europe–North America geographic dispersal of earliest Eocene primate *Teilhardina* during the Paleocene–Eocene thermal maximum. *Proc Natl Acad Sci*, **103**: 11223–11227
- Solé F, Gheerbrant E, Amaghaz M et al., 2009. Further evidence of the African antiquity of hyaenodontid (‘Creodonta’, Mammalia) evolution. *Zool J Linn Soc*, **156**: 827–846
- Sun B, Yue L P, Wang Y Q et al., 2009. Magnetostratigraphy of the early Paleogene in the Erlian Basin. *J Stratigr*, **33**: 62–68 (in Chinese with English summary)
- Swofford D L, 2002. PAUP. Phylogenetic Analysis Using Parsimony, Version 4.0b10 (Altivec). Sunderland, MA (USA): Sinauer Associates
- Szalay F S, 1969a. The Hapalodectinae and a phylogeny of the Mesonychidae (Mammalia, Condylarthra). *Am Mus Novit*, (2361): 1–26
- Szalay F S, 1969b. Origin and evolution of function of the mesonychid condylarth feeding mechanism. *Evolution*, **23**: 703–720
- Ting S Y, 1998. Paleocene and early Eocene land mammal ages of Asia. *Bull Carnegie Mus Nat Hist*, **34**: 89–123
- Ting S Y, Bowen G J, Koch P L et al., 2003. Biostratigraphic, chemostratigraphic, and magnetostratigraphic study across the Paleocene–Eocene boundary in the Hengyang Basin, Hunan, China. *Geol Soc Am Spec Pap*, **369**: 521–535
- Ting S Y, Li C K, 1987. The skull of *Hapalodectes* (?Acroedi, Mammalia), with notes on some Chinese Paleocene mesonychids. *Vert Palasiat*, **25**(3): 161–186 (in Chinese with English summary)
- Ting S Y, Meng J, Li Q et al., 2007. *Ganungulatum xincunliense*, an artiodactyl-like mammal (Ungulata, Mammalia) from the Paleocene, Chijiang Basin, Jiangxi, China. *Vert Palasiat*, **45**(4): 278–286
- Tong Y S, Wang J W, 2006. Fossil mammals from the early Eocene Wutu Formation of Shandong Province. *Palaeont Sin, New Ser C*, **28**: 1–195 (in Chinese with English summary)
- Wang Y Q, Hu Y M, Chow M C et al., 1998. Chinese Paleocene mammal faunas and their correlation. *Bull Carnegie Mus Nat Hist*, **34**: 89–123
- Wang Y Q, Meng J, Ni X J et al., 2007. Major events of Paleogene mammal radiation in China. *Geol J*, **42**: 415–430
- Woodburne M O, Swisher C C, 1995. Land mammal high-resolution geochronology, intercontinental overland dispersals, sea level, climate, and vicariance. In: Berggren W A, Kent D V, Aubry M-P et al. eds. *Geochronology, Time Scales and Global Stratigraphic Correlation*. SEPM Spec Publ, **54**: 335–364
- Zhou X Y, Gingerich P D, 1991. New species of *Hapalodectes* (Mammalia, Mesonychia) from the early Wasatchian, early Eocene, of northwestern Wyoming. *Contrib Mus Paleont Univ Mich*, **28**: 215–220

Appendix 1 Characters for the phylogenetic analysis of Mesonychia and potential outgroups (expanded and modified from the data matrix of Geisler and McKenna, 2007)

1. Size of postglenoid foramen (ordered): large (0); similar in size to fenestra vestibuli (1); absent (2).
2. Posttemporal canal (for arteria diploetica magna, also called percranial foramen): present (0); absent (1).
3. Epitympanic sinus in squamosal: present, situated in anterolateral corner of the roof of the middle ear (0); absent (1).
4. Shape of tegmen tympani: forms lamina lateral to facial nerve canal (0); inflated (1).
5. Fossa for tensor tympani muscle: shallow, anteroposteriorly elongate fossa (0); circular pit (1).
6. Perilymphatic foramen: situated in wide fossa (0); not in a fossa (1).
7. Articulation of pars cochlearis with basisphenoid/basioccipital: present (0); absent (1).
8. Ectotympanic part of the meatal tube (ordered): absent (0); present but short (1); present and long (2).
9. Posterior edge of squamosal: flat (0); sharply upturned (1); sharply upturned and bears dorsally projecting process (2).
10. Sagittal crest (ordered): absent or barely present (0); small (1); substantial (2); dorsally expanded (3).

11. Dorsal edge of braincase, relative to occlusal plane; slopes posterodorsally (0); approximately level (1); curves posteroventrally (2).
12. Foramen magnum (ordered): large, maximum dorsoventral diameter > 28% the basicranial width at the level of the external auditory meatus (0); intermediate, 24% > foramen magnum height > 15% the basicranial width (1); small, foramen magnum height < 14% the basicranial width (2).
13. Separation between occipital condyles (ordered): very large, ventral gap between condyle > 74% of maximum basioccipital width (0); large, 64% > condylar gap > 55% basioccipital width (1); moderate separation, 50% > condylar gap > 30% (2); narrow, gap < 25% basioccipital width (3).
14. Facial nerve sulcus distal to stylomastoid foramen: absent (0); anterior wall of sulcus formed by squamosal (1); anterior wall formed by mastoid process of petrosal (2); anterior wall formed by meatal tube of ectotympanic (3).
15. Length of mastoid process of petrosal (ordered): ventral portion absent (0); ventral portion short (1); elongate (2); hypertrophied (3).
16. Angle of suture of squamosal with petrosal or exoccipital, skull in ventral view (ordered): forms a 147° angle with the sagittal plane (0); forms an angle between 127° and 125° (1); angle between 111° and 105° (2); angle < 100° (3).
17. Length of external auditory meatus of the squamosal (ordered): absent (0); very short, transverse “length” of meatus < 12% the basicranial width at the level of the meatus (1); intermediate, 15% < meatus length < 20% basicranial width (2); long, 20% < meatus length < 23% (3); very long, meatus length > 26% of basicranial width (4).
18. Edge of external auditory meatus: with skull in lateral view, the dorsal edge is nearly flat (0); edge is bowed dorsally (1).
19. Glenoid fossa (ordered): in same plane as basisphenoid and basioccipital (0); slightly ventral to these bones (1); far ventral to these bones (2).
20. Preglenoid process: absent (0); present (1).
21. Foramen ovale: anterior to glenoid fossa (0); medial to glenoid fossa (1).
22. Zygomatic portion of jugal: directed postroreolaterally (0); directed posteriorly (1).
23. Alisphenoid canal (alar canal): present (0); absent (1).
24. Contact of frontal and maxilla in orbit: absent (0); present (1).
25. Postorbital process of jugal (ordered): absent (0); present, but does not contact frontal (1); with frontal forms a postorbital bar (2).
26. Ventral edge of orbit: projects dorsally (0); flared laterally (1).
27. Position of orbit relative to toothrow (ordered): over P4 or P4/M1 division (0); over M1 or M1/M2 division (1); over M2 or M2/M3 division (2); over or posterior to M3 (3).
28. Lacrimal foramina: two (0); one (1).
29. Elongation of the face (ordered): face short (0); intermediate in length (1); long (2).
30. Anterior opening of infraorbital canal: over M1 or P4 (0); at level between P3 and P4 (1).
31. Lateral surface of maxilla: flat or slightly concave (0); highly concave (1).
32. Posterior edge of nasals: terminate anterior to orbit (0); terminate posterior to the anterior edge of the orbit (1).
33. Palate: flat (0); vaulted (1).
34. Embrasure pits on palate: absent (0); present (1).
35. Angular process of mandible: no dorsal hook (0); dorsal hook present (1).
36. Medial inflection of mandibular angle: absent (0); present (1).
37. Height of coronoid process (ordered): low (0); high (1), very high (2).
38. Deep concavity on lateral surface of mandible between condyle and coronoid process of dentary: absent (0); present (1).
39. Ramus of mandible: approximately same dorsoventral thickness from m1 to m3 (0); deepens posteriorly from m1 to m3 (1).
40. Number of lower incisors (ordered): three (0); two (1); one (2).
41. Lower incisors: apex of cusp pointed or narrower than base (0); spatulate (1); peg-shaped (2); tusk-like (3).
42. P1: absent (0); present, one-rooted (1).
43. P3 roots: three (0); two (1).
44. P4 metacone (ordered): absent (0); metacone present, connate with paracone (1); metacone present, widely separated from paracone (2).
45. P4 entocingulum: present (0); absent or very small (1).
46. Styler shelves: present, occur on anterolateral and posterolateral corners of molars (0); absent (1).
47. M1 parastyle (ordered): absent (0); weak (1); moderate to strong (2).
48. m1 metaconid (ordered): subequal to protoconid (0); smaller than protoconid (1); forms a lingual swelling on protoconid (2); metaconid absent (3).
49. Postprotocristid on m1 and m2 (ordered): absent (0); present, connects protoconid to cristid obliqua (1); present and forms a carnassial notch with cristid obliqua (2).
50. Labial edge of lower molars: with tooth in occlusal view, edge emarginated between protoconid and hypoconid (0); edge is straight (1).
51. Protoconid (ordered): anterolateral to metaconid (0); in transverse line with metaconid (1); posterolateral to metaconid (2).
52. M2 metacone (ordered): subequal to paracone (0); approximately half the size of the paracone (1); highly reduced, in-

- distinct from paracone (2).
53. m2 metaconid (ordered): subequal to protoconid (0); smaller than protoconid (1); forms a lingual swelling on protoconid (2); metaconid absent (3).
 54. m2 width (ordered): wide, maximum width > 60% the maximum length (0); intermediate width, 60% > width > 34% length (1); very narrow, width < 34% the maximum length (2).
 55. M3 (ordered): larger than M2 (0); approximately equal to M2 (1); reduced, maximum mesiodistal length < 60% the length of M2 (2); absent (3).
 56. m3 hypoconulid; protrudes as separate distal lobe (0); absent (1).
 57. Number of labial cusps on M3: three cusps (0); two cusps, metacone or metastyle missing (1).
 58. m3 metaconid (ordered): subequal to protoconid (0); smaller than protoconid (1); forms a lingual swelling on protoconid (2); metaconid absent (3).
 59. Postprotocristid on m3 (ordered): absent (0); present, connects protoconid to cristid obliqua (1); present and forms a carassial notch with cristid obliqua (2).
 60. Ectocingula on upper molars: present (0); absent (1).
 61. Paraconule of upper molars (ordered): present (0); reduced (1); absent (2).
 62. Hypocone on M1 and M2: absent (0); present (1).
 63. Lower molar paraconid or paracristid position: cusp lingual or crest winds lingually (0); cusp anterior or crest straight mesiodistally on lingual margin (1).
 64. Molar protoconid; subequal to height of talonid (0); closer to twice height of talonid or greater (1).
 65. Reentrant grooves (ordered): proximal (0); absent (1); distal (2).
 66. Talonid basins; broad (0); compressed (1).
 67. Occipital condyles; broadly rounded in lateral view (0); V-shaped in lateral view, in posterior view the condyle is divided into a dorsal and a ventral half by a transverse ridge (1).
 68. Atlantoid facet of axis vertebra; restricted in coverage (0); extended dorsally at least halfway up neural arch (1).
 69. Entepicondyle of humerus; wide (0); narrow (1).
 70. Length of olecranon process; short (0); long (1).
 71. Centrale (ordered): present and large (0); present but small (1); absent (2).
 72. Manus; mesaxonitic (0); paraxonitic (1).
 73. Proximal halves of 3rd and 4th metacarpals; separate (0); contact each other (1).
 74. Width of middle portion of second metacarpal; wide (0); constricted (1).
 75. Proximal end of 5th metacarpal; expanded laterally (0); in line with shaft, not expanded (1).
 76. Greater trochanter of femur (ordered): below level of head of femur (0); approximately same level as head of femur (1); elevated dorsally well beyond head of femur (2).
 77. Third trochanter of femur; present (0); highly reduced (1).
 78. Proximal end of astragalus (ordered): nearly flat to slightly concave (0); well grooved (1); deeply grooved (2).
 79. Astragalar canal; present (0); absent (1).
 80. Navicular facet of astragalus (ordered): convex (0); saddle-shaped (1); highly concave with V-shaped notch (2).
 81. Distal end of astragalus contacts cuboid; contact present but small (0); contact large, facet almost forms a right angle with the parasagittal plane (1).
 82. Lateral process of astragalus; present, ectal facet of the astragalus faces in the plantar direction and its distal end points laterally (0); absent, ectal facet faces laterally and its long axis is parasagittal (1).
 83. Sustentacular facet of calcaneus; open, facet primarily faces to main body of astragalus (0); faces primarily to astragalar/navicular joint (1).
 84. Ridge on plantar surface of calcaneus; absent or poorly developed (0); present and well-defined, helps define a fossa on the lateral surface of the calcaneus (1).
 85. Lateral astragalar facet on calcaneus; not in transverse line with sustentacular facet, instead closer to tip of calcaneal tuber (0); nearly aligned with sustentacular facet (1).
 86. Width of the middle portion of the second metatarsal (ordered): wide (0); constricted (1); highly compressed (2).
 87. Elongation of third metatarsal (ordered): absent (0); slight elongation (1); substantial elongation (2).
 88. Ventral edge of distal phalanges of foot; distinctly concave (0); flat (1).
 89. Distal phalanges of foot in dorsal view; phalanx compressed transversely (0); broad transversely, each phalanx is bilateral with central anteroposterior axis (1); broad transversely, each phalanx is asymmetrical (2).
 90. Metaconule on M1 and M2; absent (0); present (1).
 91. Length of paraconid on lower molars; much less than talonid length (0); roughly half of talonid length (1).
 92. Angle formed by preprotocristid and postprotocristid (or postvallid) of lower molars in buccal view; broad (0); acute (1).
 93. Lingual cusp (entoconid) on lower molar talonid (ordered): present (0); vestigial (1); absent (2).
 94. Height of protoconid of p4 relative to that of m1 (ordered): p4 protoconid significantly lower than m1 protoconid (0); similar in height (1); p4 protoconid taller than m1 protoconid (2).
 95. Length of m3 with respect to m2 (ordered): m3 significantly shorter than m2 (0); m3 similar in length to m2 (1); m3 significantly longer than m2 (2).
 96. P4 parastyle; absent (0); present (1).

97. Buccal margin of upper molars in occlusal view (ordered): rounded, buccally convex (0); straight (1); buccally invaginated, forming ectoflexus (2).

Appendix 2 Character-taxon matrix for the phylogenetic analysis of Mesonychia and potential outgroups (expanded and modified from the data matrix of Geisler and McKenna, 2007)

Explanations: A = 0 + 1, B = 1 + 2, C = 0 + 3, D = 2 + 3, E = 1 + 2 + 3

<i>Arctocyon</i>	1010000?13	0??C111011	11?0001121	011000?100	?000010010
	1000200010	0100100?00	2???000010	0000020011	0002002
<i>Diacodexis pakistanensis</i>	010?1??A?1	100?012000	11011?2101	?0?0102100	1100111000
	1000100000	0000101A?0	20011B1202	11??1?1001	0002201
<i>Diacodexis metsiacus</i>	010?1?1???	?1?200100?	??0??????1	?110???10?	1?00111000
	1000100000	000010111?	?????11202	1111112101	0001201
<i>Eoconodon</i>	00101?1?12	121C122011	001?002?00	0110101?02	?0000100?0
	0000200000	1100?0?0?0	?????11?	?0?00????1	0001102
<i>Andrewsarchus</i>	0??????2	A20?234?21	101?113?11	0?10???10?	?00?010???
	?0?0?0?0?	00????0???	???????????	??????????1	?????02
<i>Hapalodectes hetangensis</i>	000?0?0?00	1??C000?01	1011210101	000101?0?	?11??12121
	211B11??21	211101????	???????????	??????????0	1122A10
<i>Hapalodectes leptognathus</i>	???????????	???????????	??????D??1	0?01???10?	?1?2112221
	212B110221	211101?0?	???????????	??????????0	102?211
<i>Hapalodectes dux</i>	???????????	???????????	???????????	??????????0	1?????121
	2?11?1?12?	??1101????	???????????	???????????	00121??
<i>Hapalodectes paleocenus</i>	???????????	???????????	???????????	??????????0?	?????????21
	2?21?1?22?	??1101????	???????????	???????????	001?2??
<i>Hapalodectes huanghaiensis</i>	???????????	???????????	???????????	???????????	??????12121
	2111?1???1	211101????	???????????	??????????0	112?1?0
<i>Hapalodectes serus</i>	???????????	???????????	???????????	0?01???????	???2?12?21
	??31?????1	211101????	???????????	??????????0	102??11
<i>Dissacus praenuntius</i>	B0?1?1???	???2132?1	0???????????	???0?1?0?	???1002121
	2111211120	201121????	???????????	???1?????0	01B0011
<i>Dissacus navajovius</i>	1??1???????	??????D??1	00??0011?1	??01???10?	??01002021
	11A1211120	201121000?	????????111	00011????0	0120011
<i>Dissacus argenteus</i>	???????????	???????????	???????????	??????????0?	?????02121
	2?11?10111	201121????	???????????	??????????0	01100??
<i>Dissacus wilwoodensis</i>	???????????	???????????	???????????	??????????1?	???002121
	2111210120	201121????	???????????	??????????1	0110011
<i>Ankalagon</i>	1?0???????	??????????1	0???????????	???000101	??01?02221
	21012111B0	201121?00?	00000A0111	00011????0	0120010
<i>Dissacus zanabazari</i>	100?111?0?	?01?A22011	0?1??011?1	0101??E100	1001002021
	21012110?0	201121000?	0110110111	001110???0	0110012
<i>Sinonyx</i>	20?1?0213	0131123121	??10002001	11000?1000	000A002221
	??112112B0	2011210???	???????????	??????????0	0121000
<i>Pachyaena gigantea</i>	?0?????20D	0???23D1B1	0???0?20A1	1?1001000?	?A11002221
	21212112B0	2011210011	11000??112	00?11??111	0121?01
<i>Pachyaena ossifraga</i>	?0?1?????1D	???2B34121	001?A02101	1110011101	?011002221
	2121210220	2011210011	1100020112	0011100111	0121101
<i>Mesonyx</i>	2011101213	1121134121	001?0?2101	?11001?111	00A1012221
	?12131?221	2011210111	0111110102	001110?110	0121011
<i>Synoplotherium</i>	20?????213	113?134121	001?002100	?110010102	?????12B21
	2121210??1	?01121??11	1100110?02	00??00011A	0121012
<i>Harpagolestes</i>	?0?????213	0121134121	101?102110	111A010001	?011012?21
	?2B031?B11	2011210?11	A?1?0?0???	??????????0	0121001
<i>Hapalodectes anthracinus</i>	???????????	???????????	???????????	???????????	???????321
	??32???3??	??1101????	???????????	???????????	112????